A Systematic Quantum Chemical Investigation of the C–H Bond Activation in Methane by Gas Phase Vanadium Oxide Cation VO^+

MIKHAIL PYKAVY,* CHRISTOPH VAN WÜLLEN
Sekretariat C3, Institut für Chemie, Fakultät II, Technische Universität Berlin, Straße des 17. Juni 135, D-10623 Berlin, Germany

Received 30 November 2005; Revised 8 August 2006; Accepted 6 October 2006
DOI 10.1002/jcc.20584
Published online 3 May 2007 in Wiley InterScience (www.interscience.wiley.com).

Abstract: The interaction between a methane molecule and the VO^+ cation in the gas phase has been investigated by means of single reference density functional (B3LYP) and wave function-based multireference (MR) correlation calculations. For the latter, an extrapolation technique is used to evaluate correlation energies at the basis set limit. A comprehensive picture for the C—H activation features a variety of molecular structures corresponding to both minima and transition states. Possible reaction paths are discussed, also taking into account change of the spin multiplicity. Activation of the methane molecule by VO^+ is always an endothermic process. Competing reaction paths might be expected. An evaluation of miscellaneous computational methods is performed using calculated energy differences for various molecular structures. Results obtained from the MR calculations exhibit no systematic convergence with increasing size of the active space used, and for two largest active spaces relative energies still differ by up to 25 kJ/mol. Simple mean difference between the B3LYP results and the best MR values is -50 ± 19 kJ/mol.

 J Comput Chem 28: 2252–2259, 2007

Key words: multireference correlation calculation; extrapolation to the basis set limit; vanadium oxide cation; alkane; CH activation

Introduction

Reactions between alkanes and supported vanadium oxide catalysts have been one of the most studied chemical processes for many years.[1] Experimental and quantum chemistry groups have made a lot of efforts to unravel the mechanisms of these complicated reactions.

Reactions between small gas phase metal oxide species and alkanes allow a deep insight into these reaction mechanisms and serve therefore as model systems for real catalysts.[2–5] An activation of the C—H bond is obviously the very first step in all such processes. However, already the interaction between a metal oxide cation MO^+ with methane is supposed to undergo a variety of different reaction paths leading to different products.[6,7] Therefore, a systematic approach is indispensable to obtain a picture of any particular system as complete as possible.

Published theoretical results in this field have been obtained from density functional (DFT) calculations, which might be considered as being semi-empirical for the most popular exchange-correlation functionals in current use. Since accurate experimental data are still being scarce for these reactions, calibration and validation of DFT methods for transition metal oxides chemistry is far from being complete.

Our experience with bare vanadium oxide species[8,9] reveals that DFT calculations provide good molecular structures (geometries), but it must be taken with caution if energetic data is concerned. Therefore we decided to start a series of high level quantum chemical investigations on the gas phase interaction of vanadium oxide cations with small hydrocarbons. Such systems have been investigated experimentally,[10] or by means of DFT calculations,[3,11] or both.[12–17] However, those studies are mostly limited to a few selected reaction paths, i.e., no systematic picture of the vanadium oxides mediated C—H activation in alkanes has been obtained so far.

In the present study we systematically investigate the interaction of VO^+ with methane. Our goals are (1) to get an exhaustive

*Present address: Berlin-Chemie AG, Glienicker Weg 125, 12489 Berlin

Cartesian coordinates for all considered molecular structures as well as table with energies calculated by means of different methods and using different basis sets are available free of charge via the Internet at http://pubs.acs.org

Correspondence to: Christoph van Wüllen; e-mail: christoph.vanwullen@tu-berlin.de

Contract/grant sponsors: Sonderforschungsbereich 546 der Deutschen Forschungsgemeirschaft and Fonds der Chemischen Industrie

description of the potential energy surfaces (PES) involved and (2) to asses the performance of DFT methods for various reaction paths on that PES as compared with our wave function-based multireference correlation calculations.

We will put our emphasis on technical part of our studies and investigate dependence of calculated energy differences on such parameters like (a) size of the active space used in the optimization of the multiconfiguration reference function and (b) method to take dynamical correlation effects into account. High level electron correlation calculations based on multi configuration reference wave functions are by no means routine. It is hard to obtain a balanced description of all different molecular structures that we present in our study. We will show how to meet with these obstacles and get reliable results.

Details of the Calculation

Density Functional Calculations

All molecular structures presented in this article have been completely optimized in the framework of spin unrestricted density functional (B3LYP) method.[18–21] Note, however, that we use the so called VWN5 functional for the local correlation part of B3LYP[22] since this is how B3LYP is implemented in most of the quantum chemical codes.

DFT calculations are mainly performed for the triplet state, which is the ground state of the methane/VO^+ encounter (van der Waals) complex. However, some of the considered species prefer quintet or singlet states, some other species can have (almost) degenerate states of different spin multiplicity. Therefore molecular structures for several spin states have been obtained in such cases.

All molecular structures have been obtained using the cc-pVTZ basis sets.[8,23] Vibrational analysis and reaction path following calculations are used to classify and validate located critical (i.e. zero gradient) points of the PES. These B3LYP molecular structures are then used for single point energy calculations at the more elaborate levels (mentioned in the following two sections). In our previous work on bare binuclear vanadium oxide clusters[9] we showed that B3LYP structures do not differ much from those obtained by means of the much more expensive MR-CI calculations. It might be desirable to optimize the molecular structures at MR-CI level, but our computational resources currently do not allow to do so.

All DFT calculations including structure optimizations, vibrational analysis, and reaction path following calculations have been performed with the Gaussian03 program (revision B.04).[24] The program has been modified to use the same version of B3LYP as found in other quantum chemistry software.[22]

Molecular Orbitals and Reference Functions

In some special cases a single Slater determinant with a well-defined occupation pattern is a good approximation to the true many-electron wave function, and occupied molecular orbitals can be obtained using the Hartree–Fock Self-Consistent Field (HF-SCF) method (see for example textbook of Szabo and Ostlund[25] for details). In many cases however, the correct wave function requires—even in a first approximation—a mixture (linear combination) of several Slater determinants with different orbital occupations. Such multiconfiguration wave function can be constructed by means of the Complete Active Space SCF (CASSCF) method.[26,27] In CASSCF, the whole molecular orbital space is divided into three subspaces: the closed shell (doubly occupied orbitals), virtual (empty orbitals), and the so called active subspace. Active orbitals have different occupations in different Slater determinants so that their averaged orbital occupation number may be anywhere between 2.00 and 0.00.

There is no general rule for the right choice of the active space.[28] First of all, we warn of the erroneous belief that larger active spaces necessarily give better wave functions. Increasing the number of active orbitals one hopes to approach, as close as possible, the desired limiting case of full configuration interaction (full CI). However, even the largest active spaces, we could handle in practice, are simply too far away from this limiting case. There is therefore little hope to observe convergence of the CASSCF wave function with the increasing active space. Moreover, in large active spaces more and more active orbitals will have occupation numbers close to 2.00 or 0.00 (say, larger than 1.95 or less than 0.05). It might be more appropriate to put such orbital to the closed shell or virtual subspace, respectively. The contribution of these very strongly or very weakly occupied orbitals to the whole wave function should be taken into account by means of the subsequent correlation calculations. Choosing active spaces is thus a delicate question which requires chemical intuition and very often a long trial-and-error way. The purpose of the present article is to report such experiment.

A strongly uniform active space for the multitude of different molecular structures we consider for CH_4VO^+ should consist of e.g. the whole valence space consisting of 22 orbitals. However, such calculations are extremely time demanding if possible at all (especially if we keep in mind calculations for larger alkanes, which we are going to address in the future). Thus, we have to use smaller active spaces, which however should be large enough to correctly and more or less uniformly describe bonding situations in all different molecular structures we want to consider.

We perform a series of CASSCF calculations (followed by multireference correlation calculations, see the following section) with active spaces of different sizes and look at the dependence of the calculated energy differences on the active space. The smallest active space consists of two molecular orbitals containing two electrons (we will indicate this active space by "(2,2)" for two orbitals with two electrons). Corresponding CASSCF calculations are equivalent to single determinant Hartree–Fock calculations for the triplet state.[†] Then we formally multiply the number of active orbitals and electrons by 2, 3, and 4, ending up with the active spaces (4,4), (6,6), and (8,8), respectively. In other words, we successively add one orbital from the closed shell space and one from the virtual space each time we enlarge the active space by a pair of electrons. We expect to "naturally" obtain active spaces consisting of pairs of bonding

[†]If N is the whole number of electrons in the system and M that of electrons in the active space, then for each molecule $(N-M)/2$ orbitals are treated as closed shell ones with the active space of a given size on top of it. This rule is valid for all CASSCF calculations presented in this article. As N remains constant in the present study, it is sufficient to give only the number of active orbitals and the number of electrons in it to completely specify individual CASSCF calculations.

and corresponding antibonding molecular orbitals. Such *a priori* definition of active spaces can be used for the whole diversity of molecular structures without a need of preliminary calculations or thresholds which would be valid for a single species (or a few of them) only.

For the active space larger than (2,2), molecular orbitals are optimized in state-averaged CASSCF calculations for the lowest triplet state and a "high-spin" state with all active electrons unpaired and ferromagnetically coupled (with weights 0.9 and 0.1, respectively). Note that the "high-spin" state is a quintet for the (4,4) active space, but a septet and a nonet for the (6,6) and (8,8) active spaces, respectively. The admixture of this "high-spin" state helps to control the nature of active orbitals: (1) it prevents often observed but undesired rotations between strongly occupied active and doubly occupied orbitals, and (2) improves the description of very weakly occupied active orbitals.

In "Reaction profile" section we will allow for states of different spin multiplicities. Their relative energies (with respect to the triplet structure of **K**) are obtained using (8,8) active space. Like just described earlier for the triplet state, molecular orbitals for each spin state are obtained from separate state-averaged CASSCF calculations for the state of the given spin multiplicity (i.e. singlet, triplet, or quintet) and the "high-spin" nonet state using weights of 0.9 and 0.1, respectively.

As mentioned above, triplet CASSCF wave functions with the (2,2) active space are equivalent to Hartree–Fock SCF wave functions, and we use them as references for single reference correlation calculations (For some molecular structures, a single Slater determinant is such a poor description that correlation calculations did not converge, see the following section). For multireference correlation calculations, molecular orbitals from the state-averaged CASSCF calculations described previously are used to construct state specific (singlet, triplet, or quintet) wave functions, which serve as reference functions. Configurations with coefficients less than a threshold of 0.01 have been omitted from the reference functions as this considerably speeds up the subsequent multireference correlation calculations but does not introduce noticeable errors.

Correlation Calculations

To take into account dynamic electronic correlation effects, i.e. short range effects which are not covered by the reference single or multi configuration wave function, we use a variety of different methods: (1) in the cases when it is possible, spin restricted single reference coupled cluster with single, double, and perturbative triple excitations, CCSD(T) (2) multireference configuration interaction with single and double excitations and Davidson correction, MR-CI + Q (3) average quadratic coupled cluster,[29] MR-AQCC (4) a hybrid of MR-CI and multireference perturbation method, CIPT2, which implies MR-CI description of all excitations from the active space and second order perturbative treatment (PT2) of all excitations involving inactive (closed shell) orbitals.[30]

Note also that we preferably use variants of the original CI method, AQCC and (much simpler) CI with Davidson correction (CI + Q), which take care of the so called size-consistency, correct scaling of calculated energies with the system size. The lack of this feature causes errors calculating energies for breaking up a molecule into fragments. Similarly, the energetics of bond breaking and bond making within a molecular complex can also be affected by this deficiency.

All valence electrons are correlated. The sub-valence 3s- and 3p-shells of vanadium have been left uncorrelated. Explicit correlation of the sub-valence electrons for $VO^{+/0/-}$ systems had minor effect on calculated binding energies.[8] We assume the same for energy differences calculated in the present study.

We use polarized correlation consistent basis sets of the triple zeta and quadruple zeta quality, cc-PVTZ and cc-pVQZ, respectively.[8,23] The correlation energies obtained for these two basis sets ($E_{\mathrm{corr}}(\mathrm{TZ})$ and $E_{\mathrm{corr}}(\mathrm{QZ})$) are then used to estimate the result at the basis set limit (BSL) by means of the two point extrapolation formula of Halkier et al.[31]

$$E_{\mathrm{corr}}(\mathrm{BSL}) \approx \frac{E_{\mathrm{corr}}(\mathrm{TZ}) \times 3^3 - E_{\mathrm{corr}}(\mathrm{QZ}) \times 4^3}{3^3 - 4^3}$$

Finally, extrapolated *total* energies are calculated as

$$E_{\mathrm{xtr}} = E_{\mathrm{CASSCF}}(\mathrm{QZ}) + E_{\mathrm{corr}}(\mathrm{BSL})$$

All related energy differences presented in our work have been calculated using the extrapolated energies E_{xtr}.

For multireference calculations we use the MOLPRO program (Versions 2002.3, 2002.8).[32]

Results and Discussion

Molecular Structures

We consider as many as possible ways to activate a single C—H bond of methane by means of the VO^+ cation in the gas phase. Figure 1

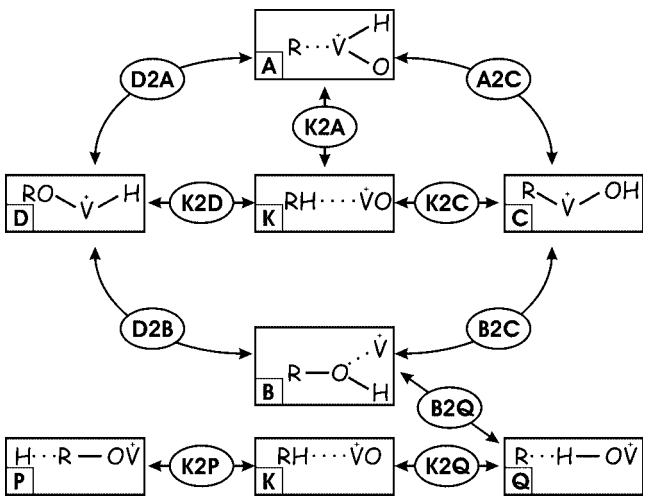

Figure 1. $VO(CH_4)^+$ species and corresponding reaction paths. Oblongs and ellipsies indicate local and transition structures, respectively.

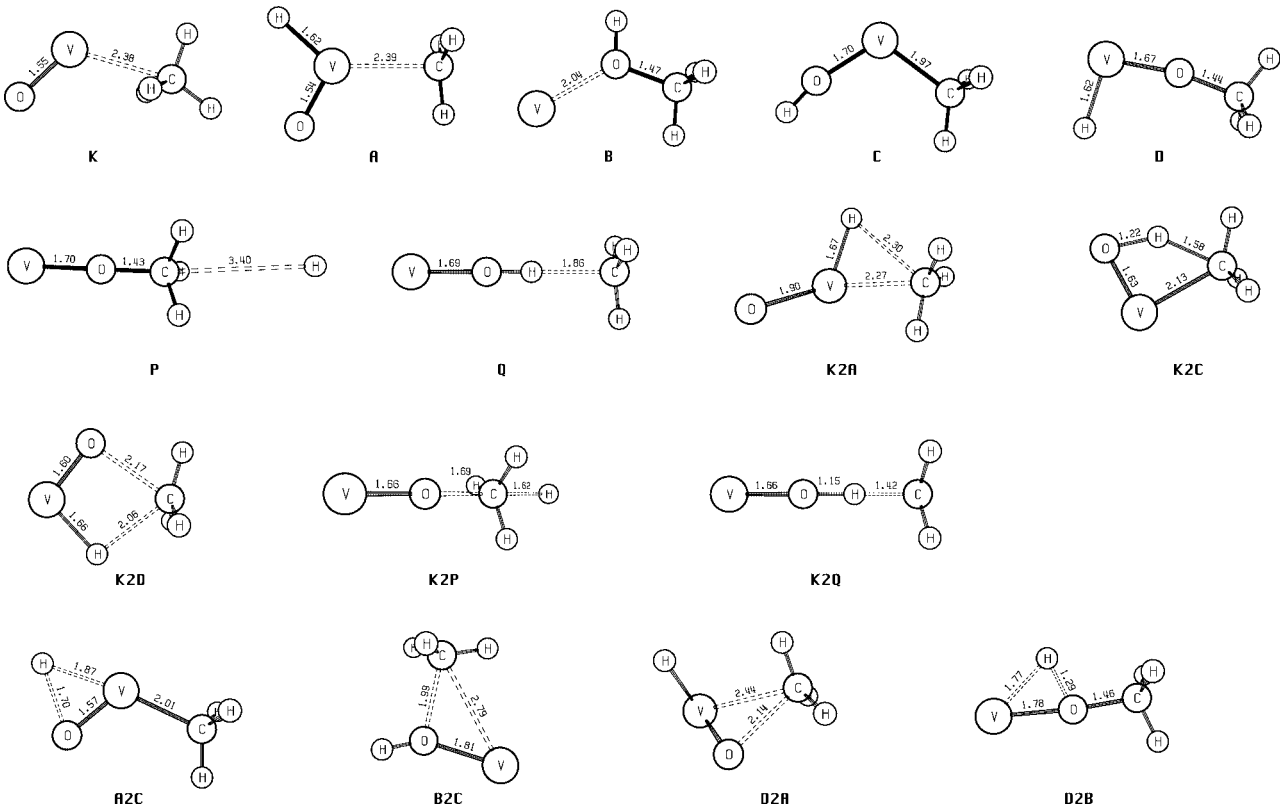

Figure 2. ORTEP plots of the molecular structures of the triplet species from Table 1 (including the encounter complex **K**). Selected bond lengths are given in Å.

shows the studied pathways,‡ and Figure 2 shows ORTEP[33] plots of these structures on the triplet hypersurface.

There are three centre interactions, which include site specific concerted insertion of either a vanadium or oxygen atom into the C—H bond which leads to a methyl hydride product **A** and a methanol–V^+ complex **B**, respectively. Reaction **K** → **A** can also be viewed as an oxidative addition at the vanadium centre which increases its formal oxidation state by two units. **K** → **B** is also known as a oxenoid insertion leading directly from an alkane to the corresponding alcohol. Another kind of a three centre reactions is the VO^+ mediated homolytic cleavage of the C—H bond leading to a pair of radicals one of which is either a hydrogen atom (pair **P**) or methyl radical (pair **Q**). Finally, there are four centre interactions which imply metathesis-type reactions giving rise to either a carbide product **C** (with a V–C bond) or a hydride product **D** (with a V–H bond), depending on the orientation of the VO^+ cation approaching the C—H bond.

Direct transitions from the encounter complex **K** to the primary products **A** through **D**, **P**, and **Q** proceed via transition states which we design by three-letter symbols like **K2A** for the passage between the structures **K** and **A** and similarly for all other structures. In addition, we also look at interconversions between the primary products: migration of either the activated hydrogen (**A** → **C**, **D** → **B**) or of the methyl group (**B** → **C**, **D** → **A**), and radical recombinations (**B** → **Q**).

Thus, we consider not only low lying intermediates and transition states, which exist along observable reaction paths but also high energy structures which are needed for the completeness of the systematic picture of the VO^+ mediated C—H activation in methane. Such systematic approach ensures that no important reaction paths could be simply forgotten. Moreover, the multitude of molecular structures is a promising playground for the comparison and accuracy assessment of different methods we want to do. A more detailed discussion of chemically relevant (i.e. low lying) reaction paths will be given in the "Reaction Profile" section.

Relative Energies from Different Methods

Table 1 reports the total electronic energies of the various minima (**A**. . .**Q**) and transition states **K2A**. . .**D2B** relative to the encounter complex **K** on triplet potential energy surface. The first two columns give the density functional (B3LYP) and coupled cluster RCCSD(T) results, the latter together with the so-called t_1 diagnostic[34] that provides a criterion whether the coupled cluster calculation is reasonable. Values above $t_1 \sim 0.06$ usually indicate that the multireference character of the wave function is large enough to deteriorate the accuracy of the coupled cluster calculation. For several structures, coupled cluster results could not be obtained due to convergence problems.

‡Cartesian coordinates of all molecular structures are available via supporting information.

Table 1. Relative Energies (kJ/mol) of $VO(CH_4)^+$ Species in the Triplet State with Respect to the Encounter Complex **K** Calculated by Different Methods.

		RCCSD(T)		MR-CI + Q				MR-AQCC	CIPT2	
Structure	B3LYP	Energy	t1[a]	(2,2)[b]	(4,4)[b]	(6,6)[b]	(8,8)[b]	(8,8)[b]	(6,6)[b]	(8,8)[b]
A	255	275	0.04	285	296	321	302	299	286	292
B	146	–	–	223	107	156	193	195	130	154
C	27	68	0.04	45	30	67	93	92	26	53
D	113	148	0.05	132	124	146	157	157	107	135
P	304	–	–	438	284	322	338	336	260	314
Q	195	–	–	356	180	223	236	235	176	212
K2A	314	290	0.05	308	300	340	324	313	300	309
K2C	169	186	0.05	188	179	187	203	207	155	183
K2D	288	323	0.06	333	336	355	357	344	303	344
K2P	364	–	–	550	382	418	431	431	359	400
K2Q	203	260	0.05	413	212	247	262	265	185	228
A2C	328	–	–	384	387	416	401	392	365	382
B2C	261	329	0.06	324	282	328	352	349	306	333
D2A	277	320	0.08	360	336	339	349	342	320	328
D2B	275	295	0.04	273	244	294	315	316	264	292

[a] t1-diagnostic of the CCSD amplitudescomputed with the cc-pVTZ basis.

[b] Size of the active space of the CASSCF reference wave function.

To clarify the source of the RCCSD(T) convergence problems, and to get more insight into the electronic structure of the species, we performed a series of CASSCF calculations with the cc-pVTZ basis set and a large active space with 8 electrons in 13 active orbitals (we will refer them "large-CAS" in further discussion). Since these large-CAS wave functions are simply too large to perform MR-CI type calculations on top of them, we cannot extract meaningful energetic data from them but rather inspect the occupation number of their natural orbitals. This shows that some of the molecular structures (**B** and adjacent transition structures **D2B**, **B2C** as well as structures associated with hydrogen abstraction **P**, **Q**, **K2P**, and **K2Q**) have four natural orbitals with occupation numbers larger than ~ 0.2. One may expect that they cannot be correctly described by a single-reference triplet wave function. This has obvious reasons: structure **B** is essentially a V^+ cation perturbed by a methanol molecule, which has a (single configuration) quintet ground state below a multi configuration triplet. Likewise, structures **P** and **Q** are biradicaloid structures with a near-degeneracy between a multideterminant triplet and a single reference quintet state.

The B3LYP and RCCSD(T) energies follow roughly the same trend for those cases where RCCSD(T) is meaningful, but in most cases the relative coupled cluster energies are 20–40 kJ/mol higher than the B3LYP results. There is no structure for which relative RCCSD(T) energy is lower than the corresponding B3LYP value. The first impression our data gives is thus that the density functional potential energy landscape is smoothed out.

This preliminary finding is further supported by the MR-CI + Q results in the following four columns, which by and large show increased energy differences compared with B3LYP. Results from different active spaces vary significantly however. On the whole, relative energies grow if the active space is enlarged. (There are exceptions especially when going from active space (2,2) to (4,4), but the large-CAS calculations demonstrate that these cases cannot be treated with the single-determinantal wave functions which result for the active space (2,2).)

For further comparison, we also document CIPT2 results for the two largest active spaces. This method is inferior to the true CI-type methods since it computes the dynamical correlation energy through a leading-order perturbative approach. Note that the dependence of the CIPT2 results on the size of the active space is of the same size compared with the native CI-type methods in contrast to the observation published in the literature that CASPT2 appears to be less sensitive to the choice of the active space[35] (CASPT2 and CIPT2 are essentially the same).

For the active space (8,8) we further show that the MR-CI + Q calculations yield results very similar to the MR-AQCC method. These two methods cover dynamical correlation effects on the basis of distinct theoretical schemes. A striking correspondence between the results from the both methods expresses confidence for evaluated correlation energies. This in turn indicates that variations of the calculated energy differences with the size of the active space are not caused by correlation methods but originate from the multi configuration reference functions which do depend on the composition of the active space. (It is also worth to mention that MR-CI + Q is much cheaper than MR-AQCC but sufficiently accurate for the applications presented here.)

To address the question whether it might be necessary to go beyond the active space (8,8), we again look at occupations of the natural orbital from large-CAS calculations. This time we used a huge active space consisting of 15 orbitals with 18 electrons, i.e. all valence electrons except for the 22 core electrons (1*s* for C and O, 1*s* through 3*p* for V) are active. We agree on that all orbitals with occupation numbers between 1.95 and 0.05 in fact belong to the active space, whereas the others should either be inactive or unoccupied, respectively. Although this recipe would lead to active

spaces of different size for different molecular structures, they never exceed the (8,8) active space. On the other side, it is less harmful to include rather weakly or strongly occupied orbitals in the active space than to omit important ones. We therefore prefer not to go below the active space (8,8).

Anyway, a common active space for *all* molecular species will occasionally be adequate for some of the cases, but at the same time it will either be too small or too large in some the other cases. This problem can hardly be avoided since it is meaningless to compare total energies from active spaces of different size, even after the MR-CI step. To quantify this uncertainty, we examine how much do calculated energies change with an increase of the active space and evaluate simple mean difference (SMD) and corresponding absolute mean deviation (given behind of the ± symbol) between the results from two consequent active spaces: a value of −62±74 kJ/mol results for the transition from (2,2) to (4,4), i.e. this transition is associated with a strong but rather unsystematic decrease of relative energies. Then we have 32±14 and 10±16 kJ/mol for the (4,4)–(6,6) and (6,6)–(8,8) steps, respectively. Note that the SMD magnitude noticeably falls whereas mean deviations level off to an almost the same value. These numbers assert the overall impression we mentioned earlier that calculated relative energies grow with increasing active spaces – SMD's are positive. By the way, we predict an SMD of −12±11 kJ/mol for the (8,8)–(10,10) step (using cc-pVTZ basis), i.e. in addition to the discussion earlier further proves that no real improvement can be expected for an active space larger than (8,8). If we take into account deviations associated with both increase and decrease of the active space (8,8), the uncertainty of the MR-CI + Q (and MR-AQCC) results for this active space adds up to 25 kJ/mol.

At last, while CCSD(T) and MR-AQCC results are similar (SMD is −19±6 kJ/mol), B3LYP values deviate significantly and less systematically from them (−31±24 kJ/mol and −50±19 kJ/mol, respectively). Thus, B3LYP energy profiles should be in any case assessed by the MR-AQCC (or MR-CI + Q) calculations. Note also that multireference correlation methods allow to calculate energies for the whole multitude of molecular species we consider, while CCSD(T) correctly converges only for the well behaved single reference cases.

Reaction Profiles

In the present section we refer relative energies of all species to the structure **K** in its triplet state and explicitly discuss results of the MR-AQCC calculations with the (8,8) active space (see Tables 1 and 2). All products of the reaction of the VO^+ cation with methane are energetically above the encounter complex **K**. Moreover, we estimate the formation energy of this complex to be 75 kJ/mol (at the RCCSD(T) level).[§] Thus, all CH_4VO^+ species considered in this work are also energetically well above the reaction asymptote $VO^+ + CH_4$ (entry channel), except for **C** which has about the same energy. MR-AQCC energy profiles for low-energy reaction paths are given graphically in Figure 3.

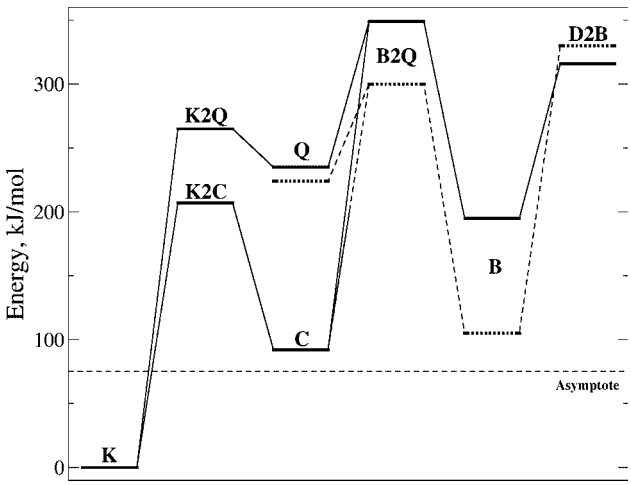

Figure 3. MR-AQCC energy profiles for low-energy reaction paths of the $VO(CH_4)^+$ system. Solid and dashed lines correspond to the triplet and quintet state, respectively. The asymptote indicates the energy of separated VO^+ and methane, calculated relative to **K** at CCSD(T) level.

In the triplet state the lowest activation energy is obtained for the reaction channel **K** → **C** with the transition barrier **K2C** of 207 kJ/mol. The result of this metathesis-type reaction is the carbide product **C** which is 92 kJ/mol above **K** and faces rather high transition barriers **A2C** and **B2C**. At first sight, no further reactions will take place on this path.

Another reaction channel with a reasonably low activation energy is the abstraction of a hydrogen atom from methane by the vanadyl oxygen, i.e. **K** → **Q**. The corresponding transition barrier **K2Q** is 265 kJ/mol and the resulting product **Q** 235 kJ/mol above the encounter complex **K**. Formed nearly separated radical pair (**Q**) can readily recombine either backwards to **K** or through a backside attack directly to the carbide product **C**.[¶] One can however imagine a stabilisation of **Q** in an environment like e.g. solid surface where another vanadyl unit can take over the methyl radical.

Pathways from **C** and **Q** to the ground state of **B** require a spin change: **B** (methanol bound to a V^+ cation) has a quintet ground state which is only 105 kJ/mol above the triplet structure **K**. A detailed discussion of such pathways would require the localization of minimum-energy crossing points between the triplet and quintet surfaces which even might play a key role in the reaction kinetics. However, in the present work we did not attempt to localize such crossing points: We can expect that the quintet states are more or less well described by a single Slater determinant, but this is not the case for the triplet states since, e.g., at **Q** and in the region around **B2C** and **B2Q** the electronic structure is biradicaloid. Although this makes the localization of triplet–quintet crossings at DFT level questionable, doing so at MR-CI level is simply a too demanding task in the present work. The transition structures **B2C** and **B2Q** might be seen as identical, as they have a similar heigth of 349 and 300 kJ/mol in the triplet and quintet states, respectively. In fact, they are situated

[§]Because it is somewhat arbitrary how to divide the active space between the fragments, it is not straightforward to calculate this energy with multireference methods. Since the complex **K** and both the fragments CH_4 and VO^+ can be described by a single Slater determinant, we calculated this interaction energy at the RCCSD(T) level.

[¶]The transition **K** → **Q** → **C** is a two step rival to the direct transition **K** → **C**. Note also, that radical recombination step **Q** → **C** is nothing else but a reverse to the streching of the C–V bond and proceeds without a barrier.

close to each other on a expanded very flat area of the PES where an almost free CH_3 unit moves around the vanadium and oxygen sites of the VOH^+ fragment.

The $2+1$ oxidative addition reaction **K** → **A** also benefits from a spin change: transition barrier **K2A** is rather high (313 kJ/mol) in the triplet state but is reduced to 216 kJ/mol in the singlet state. The singlet structure of methyl hydride product **A** is however only marginally below the transition state (215 kJ/mol) and will readily react backwards to **K** since further reactions on this path involve high transition barriers **A2C** and **D2A**. Nevertheless, the reaction **K** → **A** to which no regard was paid in the past can perfectly compete with the paths **C** → **B** or **Q** → **B** just discussed above.

All other reactions not mentioned so far (e.g. those involving species **D** or **P**) require rather high energies and are not relevant for chemistry. Therefore we do not discuss them here in detail.

In summary, methane does not react in the gas phase with the VO^+ cation unless there is an excess (collision) energy of about 200 kJ/mol. In this case the carbide product **C** and methyl hydride product **A** are accessible. Further reactions require higher energies. Except for a few $VO(CH_4)^+$ species, the triplet state turns out to be the ground state. A spin change occurs on the paths, which leads to the species **A** and **B**. However these are not felicitous examples of two state reactivity[36] when a reaction path starts in the triplet ground state of an educt, changes to (say) a singlet state at an intermediate structure and then returns to the triplet ground state of the product (spin states of the educt and the product are the same so that occured spin changes are concealed at first view). Only two step transitions like **K** → **A** → **C** can be seen as such processes which however cannot compete with direct low energy reactions (like **K** → **C**). Experimentally, no reaction between CH_4 and VO^+ has been observed at thermal collision energies.[2,10]

Finally, we shortly address the question of different theoretical methods again. As shown in the Table 2, our B3LYP results agree well with those of Shiota and Yoshizawa[3] who only investigated the path **K** → **C** → **B**. All relative B3LYP energies decrease by 10 kJ/mol on the average if zero point energy corrections are taken into account (the largest correction arises for the structure **K2Q** in the triplet state), i.e. this effect might be neglected due to much larger errors from other souces. Deviations between the CCSD(T) and MR-AQCC values do not exceed internal uncertainty of the MR-AQCC method (which is 25 kJ/mol due to the constitution of the active space), but both, CCSD(T) and MR-AQCC methods, leave to noticeably more pronounced PES landscapes in comparison to B3LYP (as already mentioned in the earlier section).

Table 2. Relative Energies (kJ/mol) for Selected $VO(CH_4)^+$ Species with Respect to the Encounter Complex **K** in its Triplet State Calculated by Different methods.

Structure	SM[a]	B3LYP		(+ZPE)	CCSD(T)	MR-AQCC
K2C	T	169	(144)[b]	158	186	207
C	T	27	(15)[b]	21	68	92
B2C(Q)[c]	T	261	(265)[b]	257	329	349
	Q	218	(221)[b]	216	266	300
B	T	146	(149)[b]	159	–	195
	Q	70	(83)[b]	83	94	105
K2Q	T	203		184	260	265
Q	T	195		183	–	235
	Q	197		185	232	224
K2A	T	314		295	290	313
	S	174		161	182	216
A	T	255		238	275	299
	S	170		160	170	215

[a] 'SM' denotes spin multiplicity: 'S', 'T' and 'Q' indicate singlet, triplet and quintet states, respectively. (Do not confuse 'Q' with the bold face '**Q**' which is used do denote molecular structure!)

[b] Taken from the work of Shiota and Yoshizawa.[3]

[c] Structures **B2C** and **B2Q** are identical, see text for details.

Conclusions

In the present quantum chemical study we extensively describe the C—H activation in the system methane/VO^+ taking into account a multitude of reaction channels after locating a large set of minima and connecting transition states. The comparison of different quantum chemical methods shows that relative energies of different CH_4VO^+ compounds have to be calculated using multireference correlation calculations. Generally we recommend stepwise extension of the CASSCF active space and extrapolation of the correlation energy towards the basis set limit. Such approach allows to validate the size of the active space in a systematic way and to overcome the slow convergence of the correlation energy with the basis set size. Correlation methods corrected for size-consistency should be favoured against the native configuration interaction method.

Since there are systematic and practical ways to overcome problems such as size consistency and slow basis set convergence, the principal remaining problem is the constitution of the active space for different molecular structures. It is demonstrated that this problem cannot be easily solved and becomes manifest in a relatively large internal uncertainty of results from multireference correlation calculations (25 kJ/mol for the (8,8) active space). Our final results are most likely of higher quality than simple density functional (B3LYP) energetic data, but involve at the same time a computational effort which is much higher.

C—H activation through a $2+2$ metathesis type insertion and subsequent formation of the carbide product **C** is the energetically favored reaction channel. Rather similar energy and a spin change from triplet to singlet requires a $2+1$ site-specific insertion giving rise to an unstable methyl hydride product **A**. A pathway starting with a hydrogen abstraction through the vanadyl oxygen involves a higher barrier but can become competitive if there is additional external stabilisation of the intermediate **Q**. Further conversions of the intermediates **C**, **A**, or **Q** as well as other reactions require larger energies and might be not of paramount interest for chemists.

Acknowledgments

The authors acknowledge HLRN for providing computer time.

References

1. Weckhuysen, B. M.; Keller, D. E. Catal Today 2003, 78, 25.
2. Schröder, D.; Schwarz, H. Angew Chem Int Ed Engl 1995, 34, 1973.

3. Shiota, Y.; Yoshizawa, K. J Am Chem Soc 2000, 122, 12317.
4. Zemski, K. A.; Justes, D. R.; Castleman, A. W., Jr. J Phys Chem A 2001, 105, 10237.
5. Zhang, G.; Li, S.; Jiang, Y. Organometallics 2004, 23, 3656.
6. Zahradnìk, R. Acc Chem Res 1995, 28, 306.
7. Xu, X.; Faglioni, F.; Goddard, III., A. W. J Phys Chem A 2002, 106, 7171.
8. Pykavy, M.; van Wüllen, C. J Phys Chem A 2003, 107, 5566.
9. Pykavy, M.; van Wüllen, C.; Sauer J. J Chem Phys 2004, 120, 4207.
10. Jackson, T. C.; Carlin, T. J.; Freiser, B. S. J Amer Chem Soc 1986, 108, 1120.
11. Gracia, L.; Andrés, J.; Safont, V. S.; Beltrán, A.; Sambrano, J. R. Organometallics 2004, 23, 730.
12. Schröder, D.; Engeser, M.; Schwarz, H.; Harvey, J. N. Chem Phys Chem 2002, 3, 584.
13. Gracia, L.; Sambrano, J. R.; Safont, V. S.; Calatayud, M.; Beltrán, A.; Andrés, J. J Phys Chem A 2003, 107, 3107.
14. Engeser, M.; Schröder, D.; Schwarz, H. Chem Eur J 2005, 11, 5975.
15. Gracia, L.; Sambrano, J. R.; Andrés, J.; Beltrán, A. Organometallics 2006, 25, 1643.
16. Feyel, S.; Schröder, D.; Rozanska, X.; Sauer, J.; Schwarz, H. Angew Chem Int Ed 2006, 45, 4677.
17. Feyel, S.; Döbler, J.; Schröder, D.; Sauer, J.; Schwarz, H. Angew Chem Int Ed 2006, 45, 4681.
18. Becke, A. D. Phys Rev A 1988, 38, 3098.
19. Becke, A. D. J Chem Phys 1993, 98, 5648.
20. Lee, C.; Yang, W.; Parr, R. G. Phys Rev B 1988, 37, 785.
21. Stephens, P. J.; Devlin, F. J.; Chabalowski, C. F.; Frisch, M. J. J Phys Chem 1994, 98, 11623.
22. Hertwig, R. H.; Koch, W. Chem Phys Lett 1997, 268, 345.
23. Dunning, H. T., Jr. J Chem Phys 1989, 90, 1007.
24. Frisch, M. J.; Trucks, G. W.; Schlegel, H. B.; Scuseria, G. E.; Robb, M. A.; Cheeseman, J. R.; Zakrzewski, V. G.; Montgomery, J. A.; Stratmann, R. E.; Burant, J. C.; Dapprich, S.; Millam, J. M.; Daniels, A. D.; Kudin, K. N.; Strain, M. C.; Farkas, O.; Tomasi, J.; Barone, V.; Cossi, M.; Cammi, R.; Mennucci, B.; Pomelli, C.; Adamo, C.; Clifford, S.; Ochterski, J.; Petersson, G. A.; Ayala, P. Y.; Cui, Q.; Morokuma, K.; Malick, D. K.; Rabuck, A. D.; Raghavachari, K.; Foresman, J. B.; Cioslowski, J.; Ortiz, J. V.; Stefanov, B. B.; Liu, G.; Liashenko, A.; Piskorz, P.; Komaromi, I.; Gomperts, R.; Martin, R. L.; Fox, D. J.; Keith, T.; Al-Laham, M. A.; Peng, C. Y.; Nanayakkara, A.; Gonzalez, C.; Challacombe, M.; Gill, P. M. W.; Johnson, B. G.; Chen, W.; Wong, M. W.; Andres, J. L.; Head-Gordon, M.; Replogle, E. S.; Pople, J. A. Gaussian 03 (Revision B.04), 2003.
25. Szabo, A.; Ostlund, N. S. Modern Quantum Chemistry: Introduction to Advanced Electronic Structure Theory, McGraw-Hill: New York, 1989. Ch. 3; 1st ed., rev. ed.
26. Werner, H.-J. Adv Chem Phys 1987, 69, 1.
27. Roos, B. O. Adv Chem Phys 1987, 69, 399.
28. Schmidt, M. W.; Gordon, M. S. Annu Rev Phys Chem 1998, 49, 233.
29. Szalay, P. J.; Bartlett, R. J. Chem Phys Lett 1993, 214, 481.
30. Celani, P.; Werner, H.-J. J Chem Phys 2000, 112, 5546.
31. Halkier, A.; Helgaker, T.; Jørgensen, P.; Klopper, W.; Koch, H.; Olsen, J.; Wilson, A. K. Chem Phys Lett 1998, 286, 243.
32. Amos, R.; Bernhardsson, A.; Berning, A.; Celani, P.; Cooper, D.; Deegan, M.; Dobbyn, A.; Eckert, F.; Hampel, C.; Hetzer, G.; Knowles, P.; Korona, T.; Lindh, R.; Lloyd, A.; McNicholas, S.; Manby, F.; Meyer, W.; Mura, M.; Nicklass, A.; Palmieri, P.; Pitzer, R.; Rauhut, G.; Schütz, M.; Schumann, U.; Stoll, H.; Stone, A.; Tarroni, R.; Thorsteinsson, T.; Werner, H. MOLPRO, a package of ab initio programs designed by Werner, H.-J.; Knowles, P. J. versions 2002.3/2002.8, 2002/2004.
33. Burnett, M. N.; Johnson, C. K. Ortep-III: Oak Ridge Thermal Ellipsoid, Plot Program for Crystal Structure Illustrations, Oak Ridge National Laboratory: Oak Ridge, TN, 1996.
34. Lee, T. J.; Taylor, P. R. Int J Quantum Chem Symp 1989, 23, 199.
35. Abrams, M. L.; Sherill, C. D. J Phys Chem A 2003, 107, 5611.
36. Schröder, D.; Shaik, S.; Schwarz, H. Acc Chem Res 2000, 33, 139.